ISSN 1819-7140, Russian Journal of Pacific Geology, 2013, Vol. 7, No. 6, pp. 384–402. © Pleiades Publishing, Ltd., 2013.
Original Russian Text © A.S. Vakh, O.V. Avcheko, V.I. Kiselev, S.A. Sergeev, S.L. Presnyakov, 2013, published in Tikhookeanskaya Geologiya, 2013, Vol. 32, No. 6, pp. 20–39.

U–Pb Isotopic Geochronologic Investigations of Zircons from Granites and Ore-Bearing Metasomatites of the Berezitiovoe Gold–Polymetallic Deposit (Upper Amur Region)

A. S. Vakh[a,b], O. V. Avcheko[a], V. I. Kiselev[a], S. A. Sergeev[c], and S. L. Presnyakov[c]

[a] *Far East Geological Institute (DVGI DVO RAN), Far East Branch, Russian Academy of Sciences, pr. Stoletiya Vladivostoka 159, Vladivostok, 660022 Russia*

E-mail: vakh@fegi.ru, sirenevka@mail.ru

[b] *Far East Federal University, ul. Sukhanova 8, Vladivostok, 690950 Russia*

[c] *Center of Isotopic Investigations, Karpinsky All-Russia Research Institute of Geology (VSEGEI), pr. Srednii 74, St. Petersburg, 199106 Russia*

Received September 11, 2012

Abstract—The results of the U–Pb geochronologic studies of zircons from the ore-bearing metasomatites of the Berezitovoe deposit in the Upper Amur region and the porphyroid biotite–hornblende host granites of the Khaikta–Orogzhan massif, which were previously considered as Early Proterozoic magmatic formations of the Late Stanovoi Complex, are examined. The SHRIMP-II and LA-ICP-MS methods were used for this purpose. It was revealed that the mass spectrometer method coupled with a laser ablation system yields precise U-Pb rock dating, and its results are comparable with the data obtained by the SHRIMP-II method. The weighted average isotopic ages are 344–355 and 323–366 Ma as established for the zircons from the porphyroid granites of the Khaikta–Orogzhan massif and from the ore-bearing metasomatites of the Berezitovoe gold–polymetallic deposit, respectively. The data definitely indicate that the metasomatites were developed after the granitoids of the Khaikta–Orogzhan massif and belong most likely to an autonomous Late Paleozoic magmatic complex. Coeval Paleozoic magmatic complexes are widespread within the Selenga–Stanovoi superterrane in the eastern and western Transbaikal regions.

Keywords: isotopic geochronology, U–Pb method, zircon, granite, gold–polymetallic deposit, North Asian craton, Upper Amur region

DOI: 10.1134/S1819714013060067

INTRODUCTION

The highly metamorphosed Aldanian and Stanovian complexes of the Stanovoi region and Selenga–Stanovoi orogenic belt bordering in the southeast the North Asian craton [6] host different-age (from the Early Proterozoic to Mesozoic) intrusions. Their formation reflects the complex polycyclic geological evolution of the marginal salients of the craton basement and its surrounding folded structures, which suffered repeated structural reorganizations and magmatic reworking during the Proterozoic and Phanerozoic [11, 12]. The main processes that determined the formation of the different-age granitoids were represented by the Early Proterozoic metamorphism and the granitization of the Precambrian complexes [37] as well as the accretionary–collisional interaction between the Siberia and Mongolia–China continents [13, 14, 27].

The oldest, Early Proterozoic granitoids are typical rocks of all the Precambrian cratons, which were formed in their peripheral parts in response to the amalgamation of crustal terranes into the Early Proterozoic supercontinent and the accretion of the juvenile crust along the periphery [34]. In the Upper Amur region, the oldest magmatic rocks are represented by widespread granitoids of the Late Stanovoi and Tukuringra complexes developed along the Dzheltulak fault [7, 9] being localized within the eastern termination of the Selenga–Stanovoi orogenic belt and the Stanovoi domain of the Aldan–Stanovoi shield (Fig. 1). These granitoids are usually accepted with a high level of conditionality to be the Early Proterozoic in age [19].

Moreover, the granitoids of the Late Stanovoi complex are considered as representing the first phase or early subphase of the Tukuringra Complex [20].

During the last years, the existence of Early Proterozoic granites within the Stanovoi belt has been frequently questioned. The recent U–Pb geochronologic studies of the granitoids from the Late Stanovoi and Tukuringra complexes of the Dzhugdzhur–Stanovoi superterrane (the Getkan and Chubacha massifs) demonstrated that they are 140–138 Ma old [9, 22–24]. This led to the substantial revision of the previous

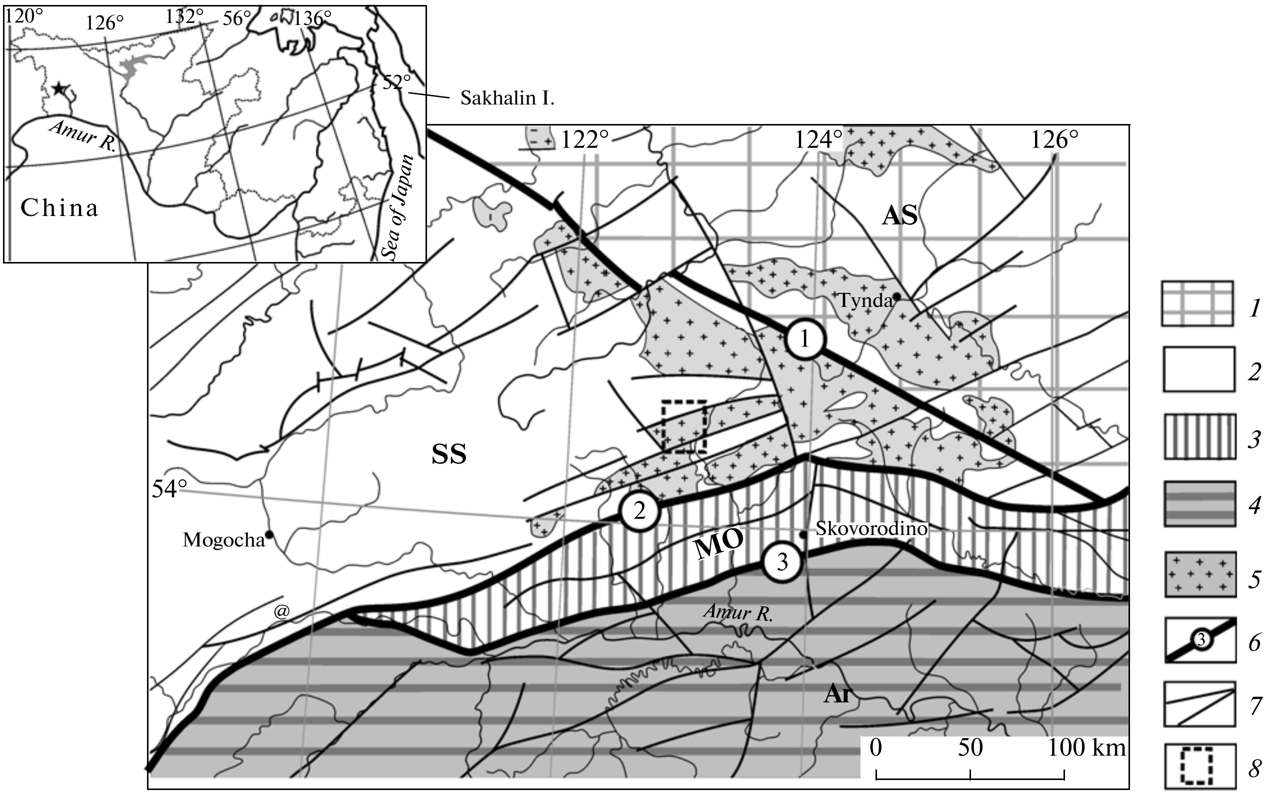

Fig. 1. Schematic distribution of the intrusive massifs of the Late Stanovoi and Tukuringra complexes in the areas adjacent to the southeastern North Asian craton. Compiled using materials from [6, 7, 9, 33].

(*1*) Aldan–Stanovoi shield (AS); (*2–4*) orogenic belts; (*2*) Selenga–Stanovoi (SS), (*3*) Mongol–Okhotsk (MO), (*4*) Argun (Ar); (*5*) granitoids of the Late Stanovoi and Tukuringra complexes; (*6*) principal regional faults: (1) Dzheltulak, (2) North Tukuringra, (3) South Tukuringra; (*7*) tectonic dislocations; (*8*) location area of the Khaikta–Orogzhon massif. In the inset, the asterisk shows the geographic position of the Berezitovoe deposit.

views on the geological evolution of the region in question and the geodynamic regime responsible for the formation of the magmatic complexes of this province. It is assumed that the formation of the Tukuringra granitoids is related to the terminal stage of the Early Cretaceous regional metamorphism of the rocks constituting the Stanovoi Group determined either by the collision between the North Asian craton and the Amur superterrane or the accretion of the Selenga–Sanovoi superterrane to the North Asian craton along the Dzheltulak fault [8, 25].

It should be noted that massifs of old granitoids of the Late Stanovoi Complex are frequently observable within the gold-ore deposits in the Upper Amur region: the Bamskoe, Kirovskoe, Berezitovoe, and others. They are particularly widespread within the Berezitovoe deposit with its ore body localized in the central part of the Khaikta–Orogzhan massif attributed to the Early Proterozoic Late Stanovoi Complex [19]. Moreover, the origin and composition of the rocks (protolith), which host the ore-bearing metasomatic zone, are still ambiguously interpreted. It is assumed that the ore zone of the deposit represents either a metasomatically reworked body of explosive breccias composed of Early Triassic subvolcanic rocks of the Desov rhyolite–trachyrhyiolite complex [3] or metasomatically altered detrital material originating from the host granitoids. Inasmuch as no distinct geological data indicating the initial composition of the protolith of the ore-bearing rocks in the deposit under consideration are available, we believe that this problem may be solved based on detailed mineralogical–geochemical investigations of the zircon (an accessory mineral that occurs both in the granites and ore-bearing metasomatites). Many isotopic investigations of zircon aggregates described in the recent geological literature unambiguously indicate that their isotopic systems remain relatively stable during thermal rock alterations [17. In this connection, zircon is the only geochronometer appropriate for dating high-temperature polymetamorphic processes, which eventually allows zirconometry to also be used for solving some specific tasks related to the genesis of ore deposits.

Thus, the geochronologic investigations of the zircons extracted from the rocks of the Berezitovoe deposit were conducted to solve two main interrelated tasks of importance for revealing the genesis of the Berezitovoe deposit, i.e., defining the nature of the protolith that served as a substrate for the formation of its ore body and establishing the age of the host granites of the Khaikta–Orogzhan massif. This work is dedicated to the results of the performed U–Pb isotopic geochronologic studies discussed below.

GEOLOGICAL DESCRIPTION OF THE KHAIKTA–OROGZHAN MASSIF AND THE BEREZITOVOE DEPOSIT

The Khaikta–Orogzhan intrusive massif is located in the interfluve of the Bol'shoi Ol'doi and Khaikta rivers (Fig. 2). In the east, north, and west, it is bordered by Mesozoic granitoids, which represent marginal fragments of the single giant Khaikta batholith with an uneven apical surface and dome-shaped sag-and-swell topography [32]. Based on the gravimetric measurements, it is assumed that the massif represents a gently southeastward dipping sheet with the shallow position of the Berezitovoe deposit's roof. In the southern part of the deposit, the Khaikta–Orogzhan massif intrudes the basement composed of Early Archean (?) and Proterozoic metamorphic intrusive ultramafic–mafic rocks. They are largely represented by biotite–hornblende gneisses and considered as representing polymetamorphic rocks of the Mogocha Group, which suffered granulite-facies metamorphism with subsequent blastomilonitization and diaphtoresis [19]. The old metamorphosed intrusive rocks referred to the Kengurak Complex of the Early Proterozoic metamorphosed gabbro [2] are represented by metagabbro, metaanorthosites, and amphibolites.

The Khaikta–Orogzhan massif is characterized by its complex heterogeneous structure. It includes the following main rock varieties: gneissose biotite–hornblende granodorites, porphyroid hornblende–biotite granites, and leucocratic biotite granites and granosyenites (Fig. 2). All these rock varieties demonstrate distinct gradual transitions between each other, which are observable in subsurface mines and boreholes drilled within the massif. Gneissose granodiorites, porphyroid granites, and leucocratic granites are considered as representing the marginal upper, intermediate, and lower deep facies of the massif, respectively.

The gneissose granodiorites are gray medium-grained rocks with pseudobanded and shadow structures. In some areas of the massif, the gneissose rock patterns are so distinct that they acquire a massive medium-grained structure and a peculiar gray-green coloration determined by the wide development of sericitization, epidotization, and chloritization. A particular feature of the granites is represented by the occurrence of large porphyroblasts of secondary microcline in granites up to 1–2 cm across, which replaces plagioclase and contains inclusions of early minerals. Leucocratic biotite granites most widespread in the northern part of the Khaikta–Orogzhan massif are represented by light medium-grained rocks consisting of K-feldspar, quartz, plagioclase, and subordinate biotite.

The Khaikta–Orogzhan massif is crossed by many dikes of aplitic granites from a few centimeters to 1–2 m thick. In addition, the porphyry- and gneissose granitoid varieties enclose abundant xenoliths of altered gabbroids from a few centimeters to a few tens of meters across belonging to the Kengurak Complex.

Recently, the granitoids of the Khaikta–Orogzhan massif have been accepted with a high level of conditionality as being the Early Proterozoic in age. This is confirmed by their similarity in petrographic and petrochemical properties with the granitoids of the Late Stanovoi Complex of the Aldan–Stanovoi shield. According to the bulk K–Ar measurements in the granitoids, the massif is 144–125 Ma old [30]. It may be assumed that the obtained dates reflect the terminal stage in the transformation of the rocks of the massif determined by the formation of the Mesozoic granitoids of the Khaikta massif.

The central part of the Khaikta–Orogzhan massif hosts the Berezitovoe deposit represented by sulfide-bearing tourmaline–granite–muscovite–quartz rocks, which form a steeply dipping body within the porphyroid granitoids (Fig. 3). In plan, the ore body of the massif exhibits a complex lenticular shape, being 900 m long at the surface and from 10–15 to 110 m thick.

The main share of ore-bearing metasomatites in the deposit is composed of relatively uniform light gray to greenish gray massive fine-grained muscovite–quartz rocks with abundant inclusions (up to >1%) of almandine–spessartine garnet and tourmaline. The rocks also contain in variable proportions orthoclase, chlorite, biotite, anorthite, Zn spinel (ferruginous gahnite), titanite, zircon, epidote, allanite, prehnite, fluorapatite, grotite, fluorite, and graphite. At the contact with the host granitoids, the ore-bearing metasomatites are fringed along their periphery by dark gray compact varieties of complex garnet–biotite–anorthite–muscovite–quartz composition, which grade into altered granites.

The distribution of the gold-bearing polymetallic ores within the tourmaline–garnet–muscovite–quartz metasomatites is relatively regular: they form a complex sulfide stockwork and distinctly fill a branched system of complex fissures. The main ore minerals are sphalerite, galenite, pyrite, pyrrhotite, and magnetite. The mineral composition of the ores is described in detail in [4].

ANALYTICAL TECHNIQUE

The composition of the rocks and minerals was analyzed at the Analytical Center of the DVGI DVO RAN. The content of petrogenic components in the rocks was estimated by applying the standard chemical analysis and measurements using the X-ray fluores-

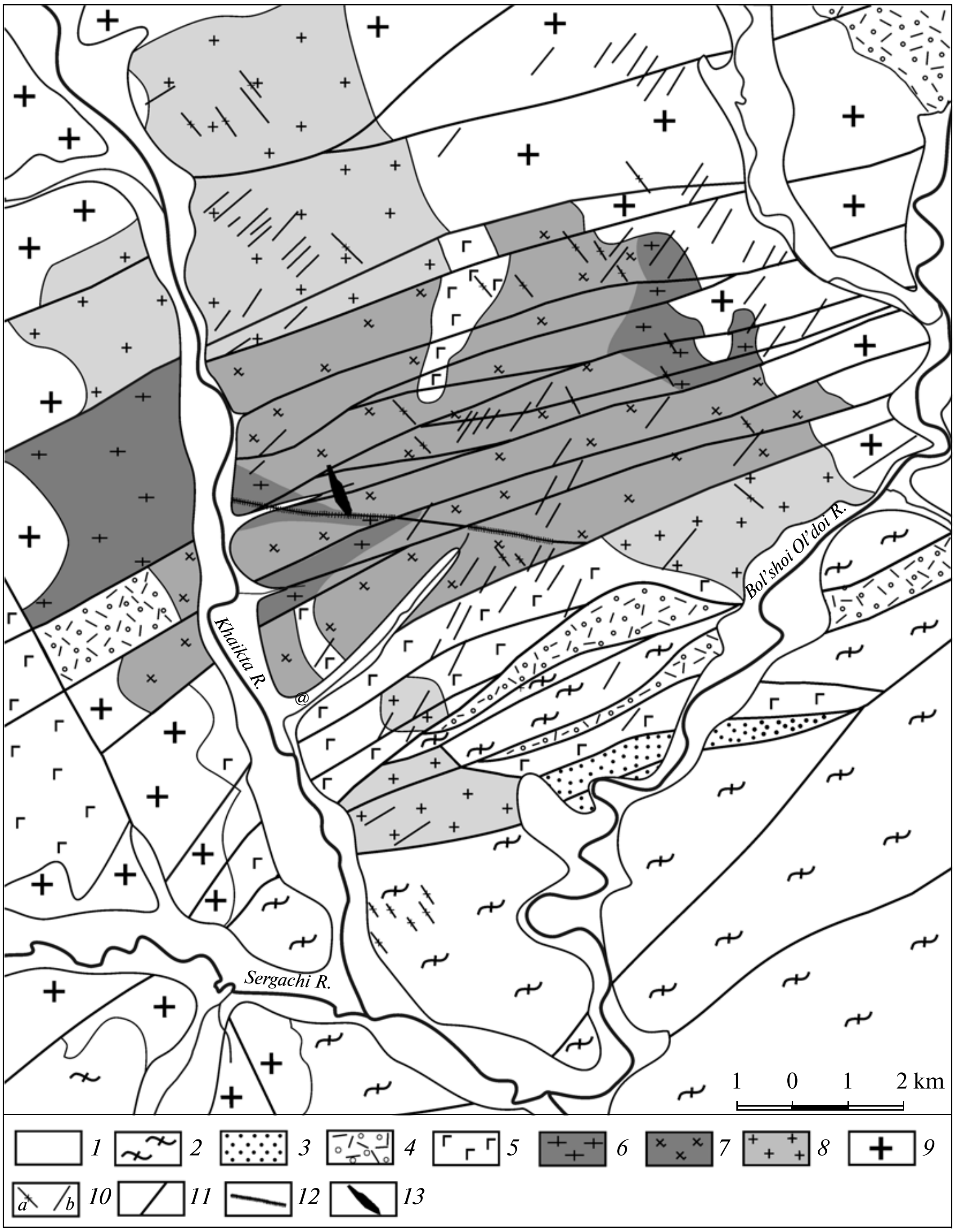

Fig. 2. Schematic geological structure of the Khaikta–Orogzhon massif. Compiled using materials of regional geological agencies.

(*1*) unconsolidated alluvial sediments; (*2*) Early Archean metamorphic rocks of the Mogocha Group: crystalline schists and gneisses; (*3*) Lower Proterozoic metamorphosed sedimentary rocks of the Early Triassic Desov Complex; (*4*) volcanogenic and volcanosedimentary: trachyrhyolites, rhyolites, rhyodacites, tuffaceous siltstones, and tuffaceous mudstones; (*5*) Early Proterozoic Kengurak mafic–ultramafic complex, after [1]: metagabbro, amphibolites, metaanarthosites, metapyroxenites; (*6–8*) Early Proterozoic (?) intrusive rocks of the Khaikta–Orogzhon massif of the Late Stanovoi Complex (?): (*6*) gneissose biotite–hornbelnde granodiorites, (*7*) porphyroid biotite–hornblende granodiorites and granites, (*8*) leucocratic biotite granites and granosyenites; (*9*) Early Cretaceous Khaikta Complex of subalkaline granitoids, after [40]: coarse-grained porphyroid biotite–hornblende granodiorites, granites, and granosyenites; (*10*) Early Cretaceous dikes: (a) granodiorite– and granite–porphyries, (b) spessartite and diorite–porphyrites; (*11*) principal tectonic fractures; (*12*) quartz veins; (*13*) Berezitovoe gold-polymetallic deposit.

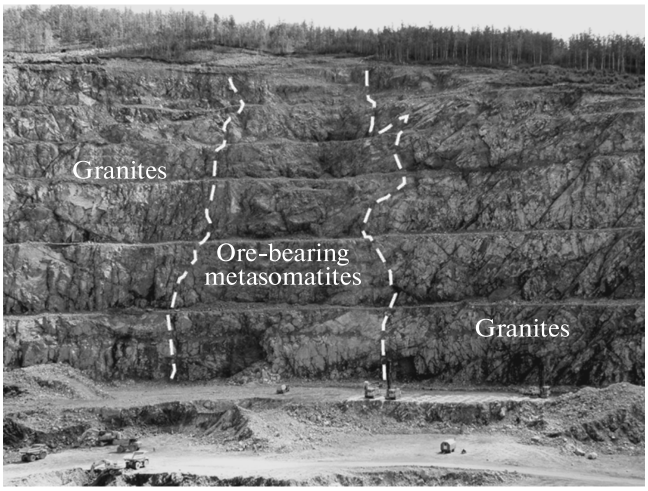

Fig. 3. Structure of the southern part of the ore zone in the Berezitovoe deposit.

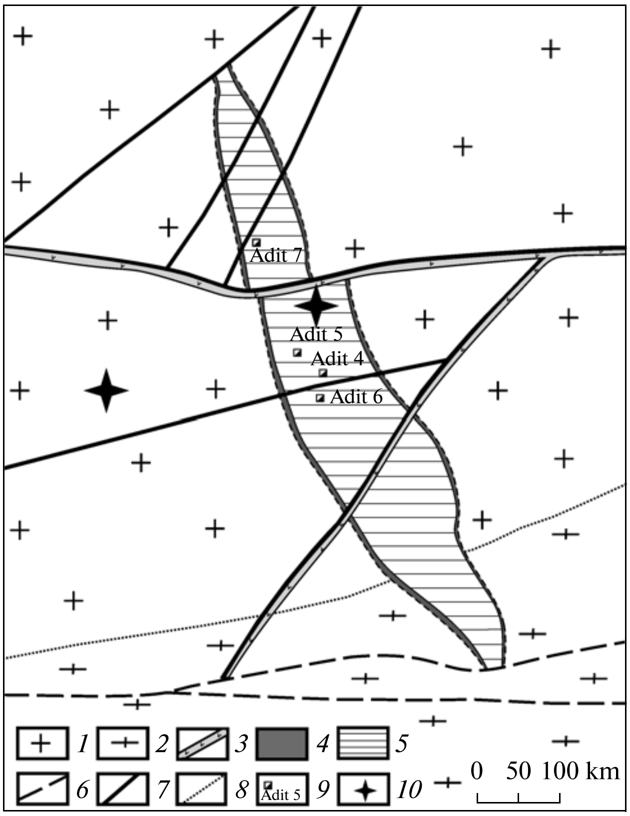

Fig. 4. Schematic map illustrating the location of the samples taken from the Berezitovoe deposit for the isotopic investigations.

(*1, 2*) Early Proterozoic (?) intrusive rocks presumably of the Late Stanovoi Complex (?): (*1*) porphyroid granites and granodiorites, (*2*) gneissose granodiorites; (*3*) Early Cretaceous spessartite and diorite–porphyrite dikes; (*4*) garnet–muscovite–biotite–orthoclase–anorthite–quartz metasomatites; (*5*) tourmaline–garnet–muscovite–quartz metasomatites with gold-polymetallic mineralization; (*6*) quartz veins; (*7*) principal tectonic fractures; (*8*) facies boundaries; (*9*) exploration adits and their numbers; (*10*) sampling sites.

cence method using a VRA-30 scanning spectrophotometer and an S4 Pioneer spectrometer. The detection limit of the elements from Na to U (VRA-30 spectrometer) and the elements from F to U (S4 Pioneer spectrometer) was 0.0005 %. The measurement accuracy was 2% for the petrogenic components in the rock; 5% for the trace elements Rb, Sr, Nb, Sc, Co, Ni, Cu, Zn, Ga, Y, Th, U, Pb, and AS; and 10% for Ba, Cr, V, La, Ce, and Nd. The REE and rare elements in the granites and meatsomatites were determined by the ICP-MS method using the Agilent 7500 equipment. The accuracy of the measurements by the ICP-MS method is determined by the value of the standard deviation, which is usually equal to 1–2% for most matrix elements, 5–15 % for most accessory elements, and 20–25 % for Hf, Th, and Pb. These values meet the quality criterions of the elemental analysis accepted in geochemical investigations.

The isotopic geochronologic investigations were conducted by the U–Pb method using single zircon grains at the high-resolution SHRIMP-II precision ionic microprobe at the Center of Isotopic Investigations of the VSEGEI and by the LA-ICP-SM method at the DVGI DVO RAN at the Agilent 7500a mass spectrometer with inductively coupled plasma combined with a UP-213 laser ablation system.

The zircons for the isotopic investigations were extracted from two volumetric rock samples from the deposit. One sample was taken from the ore-bearing tourmaline–garnet–muscovite–quartz rocks of the ore zone and the other from the host porphyroid granites (Fig. 4). The zircons were extracted from the metasomatites and granites in line with the standard procedure.

The zircons were subjected to two-stage isotopic investigations. First, the zircon grains were implanted at the Center of Isotopic Investigations (VSEGEI) onto a plate covered by epoxy together with grains of the TEMORA and 91500 zircon standards. Their internal structure was studied in the cathode luminescence regime; then, the U–Pb ratios were measured at the SHRIMP-II ion microprobe only in the marginal parts of the zoned zircon grains. The measurements were conducted in line with the technique in [51]. The intensity of the primary beam of molecular negatively charged oxygen ions was 4 nA and the crater's diameter was ~30 μm. The obtained data were processed using the SQUID and ISOPLOT/EX programs [43, 44]. The U–Pb ratios were normalized to the 0.0688 value of the TEMORA zircon standard, which corresponds to its age of 416.75 Ma [39].

The plate with the zircon grains and the standards prepared at the Center of Isotopic Investigations (VSEGEI) was forwarded to the DVGI DVO RAN for further isotopic measurements by the LA-ICP-MS method. The U–Pb isotopic ratios were largely measured by this method in both the peripheral and central parts of the zircon grains, which were previously studied by the SIMS method (secondary ion mass spectrometry) using a SHRIMP-II microprobe.

The isotopic measurements by the LA-ICP-MS method were conducted at an Aglient 7500a mass spectrometer with inductively coupled plasma and combined with a UP-213 laser ablation system. The parameters measured at the mass spectrometer were optimized for obtaining the maximal intensity of the ^{208}Pb mass using the standard sample N.I.S.T. SRM611 and fulfilling the condition that the ratio between the intensities of the masses ^{240}ThO+/^{232}Th+ < 1%. All the measurements were conducted in the regime of integration with the time resolution and measuring peaks of the ^{202}Hg, ^{204}(Pb+Hg), ^{206}Pb, ^{207}Pb, and ^{238}U masses. The intensity of the ^{238}U mass was calculated using its peak according to the natural distribution of the $^{238}U/^{235}U = 137.88$ U isotopes. Material from the sample was taken for the analysis by the laser beam at a single point. The diameter of the ablation crater was approximately 40 μm. Under the chosen parameters of the isotopic ratio measurements, the ablation crater approximately 40 μm across is deepened with a rate of 1 μm/s. The material removed by the laser from the crater was transported by the helium and argon mixture.

The main features of the technique used for measuring the isotopic ratios by the LA-ICP-MS method are described in [18, 42]. The isotopic analysis of the zircons was conducted with a series of measurements. At the beginning and end of each series, the zircons of the TEMORA [39] and 91500 [50] standards, the isotopic characteristics of which were studied by many researchers, were measured. The intermittent measurements of the TEMORA zircons at a time maximally close to the measurements of the unknown samples allowed both the isotopic fractionation stimulated by the laser beam and the discrimination according to the masses determined at the mass spectrometer to be taken into account. Zircon grains from the 91500 standard were analyzed to control the reproducibility of the obtained values and the stability of the equipment's functioning. The result of a single analysis of the isotopic ratios is an average of approximately 300 measurement cycles. Time-correlated signals clustered into intervals with their stable values (free from the influence of inclusions, core–rim transition zones, and zones with high contents of common lead), which were used in the subsequent age calculations, were obtained for each analysis. The measured values were processed using the Glitter version 4.4.2 program (Access Macquarie Ltd).

The analysis of the TEMORA standard sample yielded the weighted average $^{206}Pb/^{238}U$ age of 416.88 ± 0.93 Ma (MSWD = 0.34, $n = 64$) (the $^{206}Pb/^{238}U$ age measured by the TIMS method is 416.75 ± 0.24 Ma [39]) and a concordant age of 1062.3 ± 2.2 Ma (1σ, MSWD = 0.34, $n = 64$) for the 91500 zircon standard (the $^{206}Pb/^{238}U$ age measured by the ID-TIMS method is 1062.4 ± 0.4 Ma [50]). Diagrams with concordia were constructed using the Isoplot/Ex version 3.00 program [43].

PETROCHEMICAL AND GEOCHEMICAL PROPERTIES OF INTRUSIVE ROCKS AND ORE-BEARING METASOMATITES

Tables 1 and 2 demonstrate the respective data on the chemical composition of the intrusive rocks from the Khaikta–Orogzhan massif and the contents of trace elements in them. The SiO_2 and K_2O contents in the rocks from this massif vary from 64 to 75 and from 2.8 to 6.1 wt %, respectively. The porphyroid biotite–hornblende granites of the massif belong to the medium-K calc-alkaline series, while the other varieties are referred to its high-K counterpart (Fig. 5). In the (Na + K)/Al–SiO_2 diagram, the data points of the granites are also localized in the field of calc-alkaline rocks, except for the aplitic granites, which correspond to the alkaline series (Fig. 5). Moreover, the minimal values of the agpaitic index (Na + K)/Al are characteristic of the porphyroid granites of the massif under consideration.

In discrimination diagrams, the porphyroid and leucocratic granites, which constitute the largest part of the massif, are located in the field of granitoids of the *M*, *I*, and *S* types (Fig. 6). The REE concentrations in the rocks of the massif exhibit values comparable with their average contents in the granites from the upper part of the continental crust [46]. The porphyroid and leucocratic granites of the massif demonstrate a uniform slightly fractionated profile of the chondrite-normalized REE distribution [45] (Fig. 7). It is characterized by the enrichment with light lanthanoids and the depletion of its heavy varieties ($(La/Yb)_{cn}$ = 6–19) with a distinct Eu anomaly ((Eu/Eu*) = 0.71–0.68).

The ore-bearing metasomatites of the Berezitovoe deposit are composed of peculiar tourmaline–garnet-bearing muscovite–quartz rocks. The following main types of altered rocks are definable from the host granites toward the central part of the ore lode: slightly altered granite—intensely altered granite—"dark gray" fine-grained garnet–biotite–anorthite–muscovite–quartz metasomatites—"light gray" metasomatites largely of tourmaline–garnet–quartz composition. Tables 1 and 2 illustrate the chemical compositions of the main metasomatic rocks of the deposit and the concentrations of the main trace elements, respectively. The analysis of these data reveals that the metasomatites are characterized by lower Na, Ca, Ba, and Sr and higher K, Mn, and Rb concentrations as compared with the host granites.

The metasomatites from the marginal parts of the ore zone are characterized by higher REE concentra-

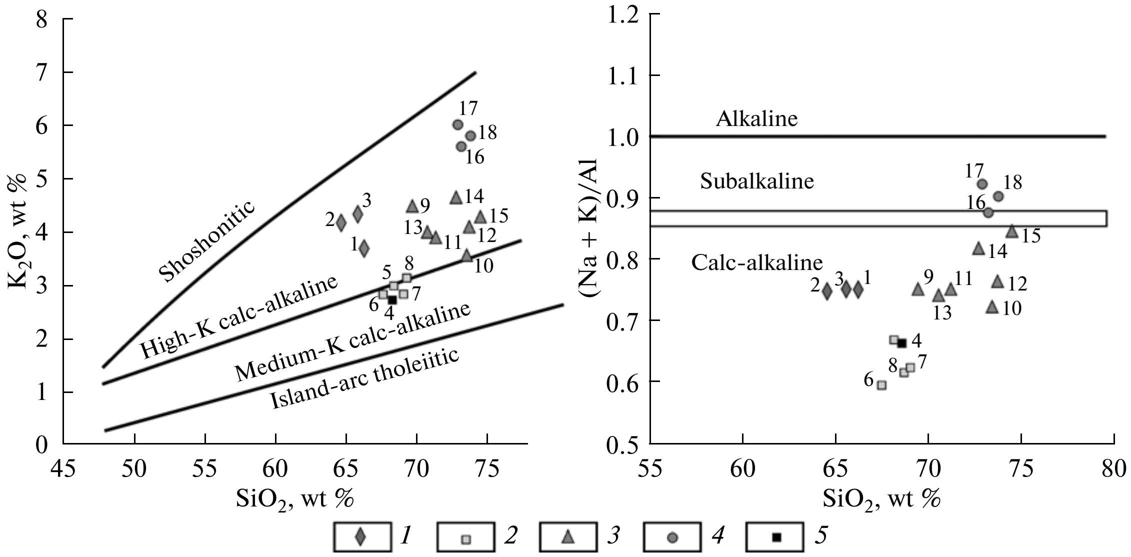

Fig. 5. SiO_2–K_2O and SiO_2(Na+K)/Al classification diagrams for the granitoids of the Khaikta–Orogzhon massif.
(*1*) gneissose biotite–hornblende granodiorites; (*2*) porphyroid biotite–hornblende granodiorites (*3*) leucocratic biotite granites; (*4*) aplitic granites; (*5*) sample of porphyroid granites used for the U–Pb isotopic investigations. The numbers of the points correspond to the sample numbers in Table 1. The fields of the magmatic series are given after [49].

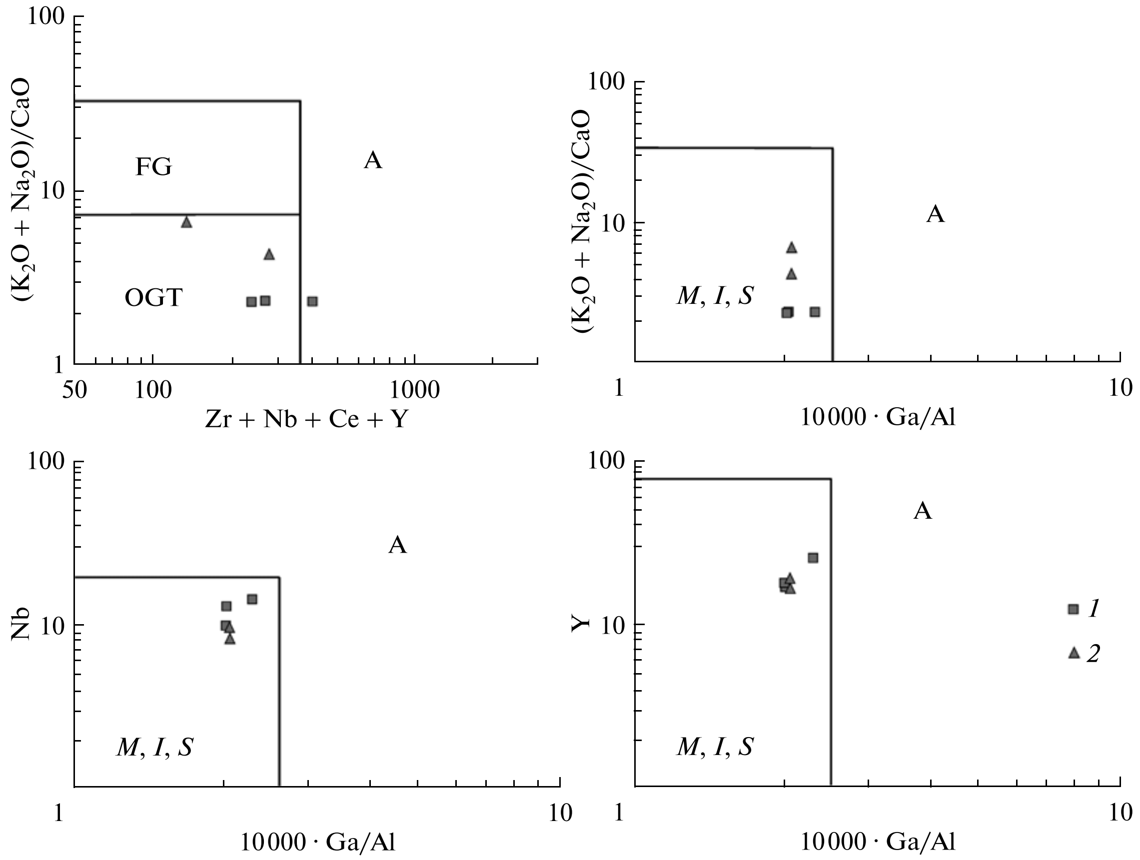

Fig. 6. Discrimination diagrams [47, 48] for the porphyroid biotote–hornblende (1) and biotite leucocratic (2) granites of the Khaikta–Orogzhon massif.
(FG) fractionated granites; (OGT) nonfractionated *M*, *I*, and *S* granites; (A) *A* granites.

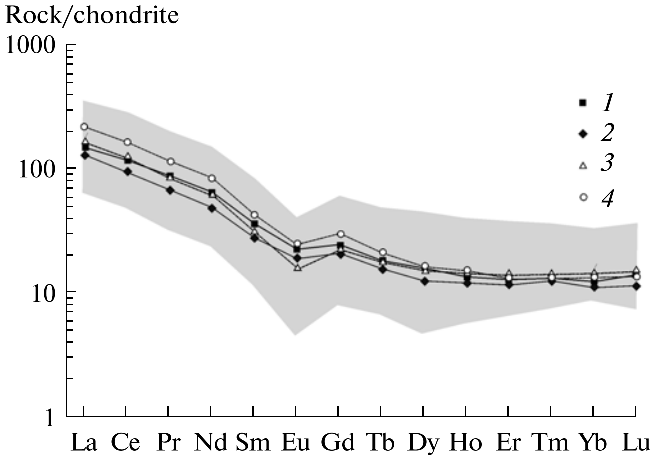

Fig. 7. REE distribution in the granites and ore-bearing metasomatites of the Berezitovoe ore field.
(*1*, *2*) granitoids of the Khaikta–Orogzhon massif: (*1*) porphyroid biotite–hornblende granites (average of three analyses), (*2*) leucocratic biotite granites (average of two analyses); (*3*, *4*) ore-bearing metasomatites of the Berezitovoe deposit: (*3*) "light" tourmaline–garnet–muscovite–quartz variety with gold–polymetallic mineralization (average of three analyses), (*4*) "dark gray" tourmaline–garnet–muscovite–biotite–orthoclase–anorthite–quartz variety from marginal parts of the ore-bearing zone (average of four analyses). The gray field corresponds to the REE variation limits in the examined samples. Normalized after [45].

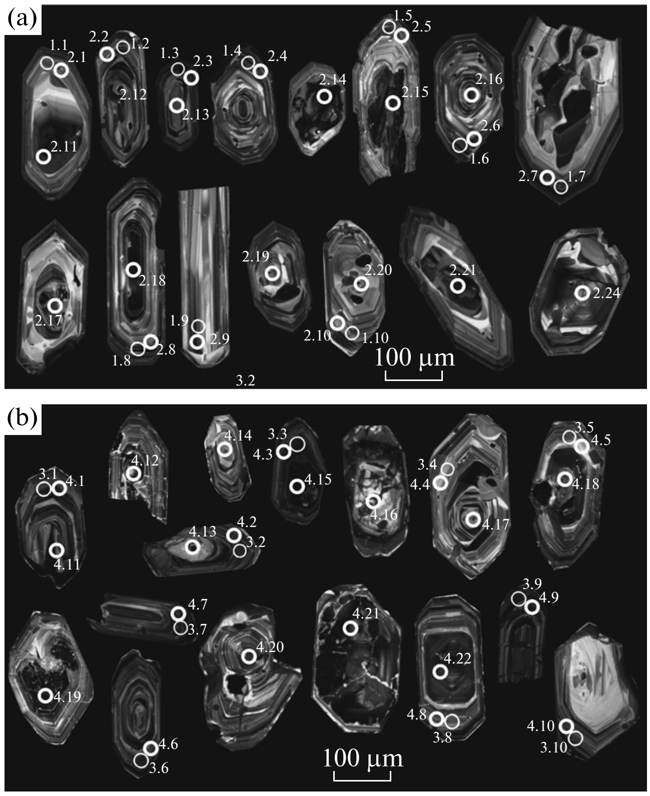

Fig. 8. Cathode luminescence images of the zircons from the porphyroid granites of the Khaikta–Orogzhon massif (A) and the ore-bearing metasomatites (B) of the Beresitovoe deposit. The circles show the measurement points. The numbers of the measurements correspond to the analysis numbers in Table 3 and 4.

tions as compared with the host granites, whereas the tourmaline–garnet–muscovite–quartz metasomatites from the main body of the ore zone exhibit their lower contents. The REE distribution in the chondrite-normalized [45] metasomatites is similar to that in the granites (Fig. 7).

RESULTS OF THE GEOCHRONOLOGIC INVESTIGATIONS OF THE ZIRCONS

By their morphology and coloration, the zircon garins from the granites and metasomatites are identical and demonstrate significant similarity between each other. They are largely represented by well faceted uniform euhedral transparent colorless to pinkish aggregates of short-prismatic to, less commonly, acicular crystals 20 to 300 μm across. The study of zircons using the JXAS8100 microprobe (DVGI DVO RAN) revealed that they contain only HfO_2 (0–1.56 %) in addition to zirconium. No other mineral inclusions are detected in the zircon grains.

The cathode luminescence images of the zircons from the granites and metasomatites show that they include well-developed cores with an unzoned or slightly zoned structure and marginal rims with fine rhythmical zoning patterns (Fig. 8).

Tables 3 and 4 present the results of the isotopic geochronologic investigations of the zircons. The weighted average age calculated from eight data points obtained by the SHRIMP-II method for the marginal rims of the zircon grains from the Khaikta–Orogzhon massif is 344.8 ± 3.3 Mq and that calculated from nine data points obtained by the LA-ICP-MS method is 344.9 ± 7.8 Ma (Fig. 9). The weighted average concordant age value calculated from 22 data points obtained for cores of zircon grains by the LA-ICP-MS method is as old as 354.8 ± 2.0 Ma. At the same time, it should be noted that the cores of the zircons also yielded older values: a weighted average concordant age of 1828 ± 42 Ma and a weighted average discordant age of 1477 ± 38 Ma. Thus, taking into consideration the data obtained by these two methods, it may be assumed that the granites of the Khaikta–Orogzhon massif are 344–355 Ma old.

According to the SHRIMP-II data, the weighted average age value for the marginal parts of the zircon grains from the ore-bearing metasomatites of the Berezitovoe deposit calculated for nine data points is 335.9 ± 4.8 Ma (Fig. 10). The weighted average age value obtained for these rocks by the LA-ICP-MS method is estimated to be 323.1 ± 7.0 Ma (based on six data points). At the same time, the zircons also yielded

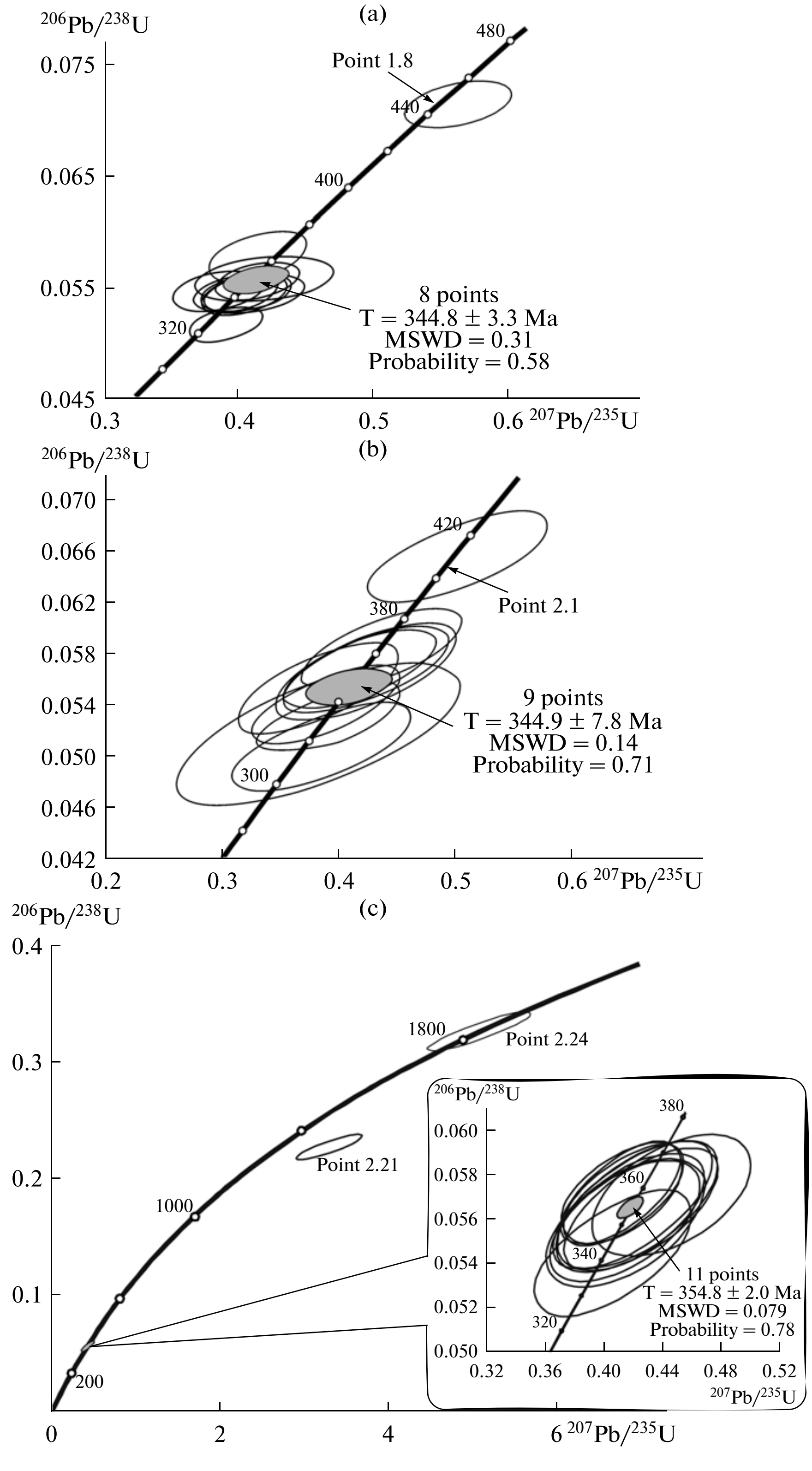

Fig. 9. Diagrams with concordias for the marginal zones (A, B) and cores (C) of the zircon grains from the granites of the Khaikta–Orogzhon massif measured by the SIMS (A) and LA-ICP-MS methods (B and C).

The inset in diagram *C* illustrates the fragment of the concordia in the age interval of 320–360 Ma. The age values for the individual isolated points are given in Tables 3 and 4.

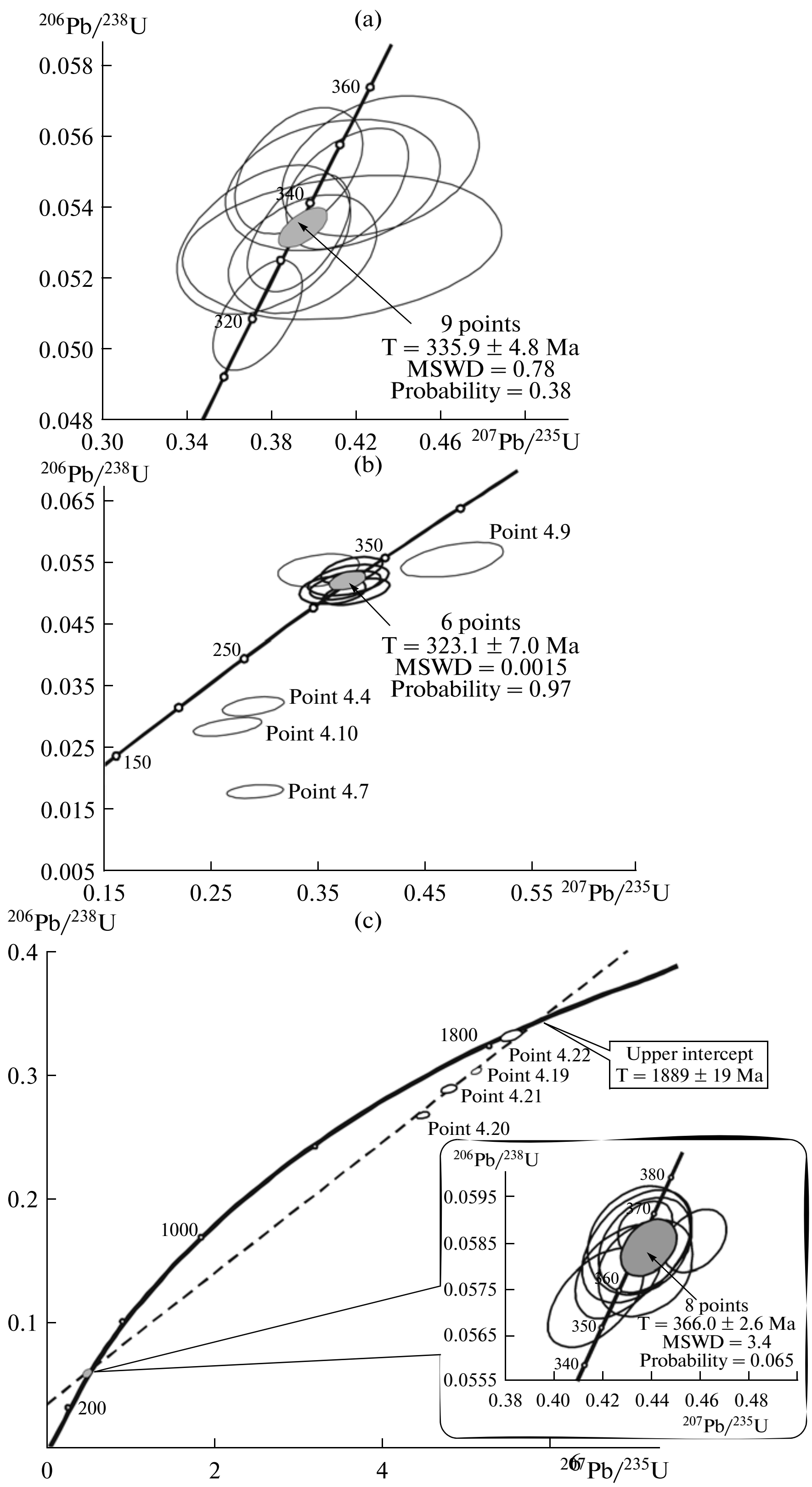

Fig. 10. Diagrams with concordias for the marginal zones (A, B) and cores (C) of the zircon grains from the ore-bearing metasomatites of the Berezitovoe deposit measured by the SIMS (A) and LA-ICP-MS methods (B and C).
The inset in diagram *C* illustrates a fragment of the concordia in the age interval of 340–380 Ma. The age values for the individual isolated points are given in Tables 3 and 4.

Table 1. Chemical composition of the granitoids of the Khaikta–Orogzhon massif and the metasomatites of the Berezitovoe deposit (wt %)

Component	213	251	386	@Âõ-1*	@Âõ-2*	309	311	426	@Âõ-3*	206	245	258	313	356	379	361	380	430/1	8-1*	65	8-2*	6*	1267
	1	2	3	4	5	6	7	8	9	10	11	12	13	14	15	16	17	18	19	20	21	22	23
SiO_2	66.24	64.65	65.73	68.71	68.32	67.62	68.86	69.13	69.57	73.62	71.26	73.84	70.7	72.84	74.6	73.32	72.96	73.92	65.47	68.36	69.42	67.63	64.71
TiO_2	0.55	0.76	0.74	0.34	0.31	0.26	0.25	0.28	0.27	0.15	0.20	0.20	0.16	0.14	0.08	0.25	0.32	0.10	0.40	0.18	0.36	0.32	0.48
Al_2O_3	14.07	15.36	14.42	15.80	16.28	16.31	15.65	16.84	15.73	13.30	13.63	13.20	14.46	13.27	13.27	13.03	12.62	13.17	16.94	15.72	17.87	18.14	17.38
Fe_2O_3	4.78	3.81	4.12	3.34	3.00	1.19	1.81	1.4	2.58	1.70	2.04	1.53	1.51	1.00	0.87	1.35	1.60	0.95	4.41	2.16	2.31	3.46	5.00
FeO	3.02	2.54	2.32	–	–	2.40	1.92	1.28	–	1.17	2.21	1.23	1.70	1.70	1.56	1.58	2.04	1.28	–	1.48	–	–	1.78
MnO	0.10	0.15	0.12	0.09	0.09	0.07	0.09	0.05	0.06	0.05	0.08	0.04	0.10	0.05	0.05	0.06	0.08	0.05	0.96	0.40	0.10	1.47	0.68
MgO	1.10	0.88	0.72	0.94	0.83	1.22	0.9	0.72	0.73	0.62	0.87	0.82	0.75	0.72	0.35	0.39	0.27	0.28	1.04	0.80	0.48	0.42	0.77
CaO	2.32	2.08	2.12	3.14	3.23	2.94	2.7	2.12	2.02	1.73	1.21	0.87	2.20	1.25	0.87	0.70	0.72	1.05	2.76	3.05	0.22	0.26	0.17
Na_2O	3.98	4.26	3.74	4.56	4.66	4.05	4.00	4.32	4.23	3.52	3.62	3.43	3.90	3.50	4.00	3.21	3.11	3.37	0.26	0.37	0.15	0.18	0.23
K_2O	3.70	4.19	4.37	2.78	3.01	2.85	2.85	3.17	4.5	3.56	3.93	4.09	4.00	4.70	4.30	5.69	6.07	5.88	5.06	6.00	5.93	5.27	6.15
H_2O^-	0.00	0.07	0.12	–	–	0.00	0.00	0.00	–	0.05	0.09	0.06	0.00	0.00	0.00	0.10	0.17	0.00	–	–	–	–	–
H_2O^+	0.20	0.28	0.34	–	–	0.3	0.43	0.2	–	0.30	0.54	0.31	0.34	0.38	0.47	0.06	0.04	0.00	–	–	–	–	–
P_2O_5	0.17	0.28	0.21	0.14	0.12	0.22	0.16	0.15	0.10	0.13	0.10	0.11	0.10	0.10	0.08	0.15	0.17	0.12	0.14	0.08	0.14	0.02	0.19
L.O.I.	0.20	0.28	0.83	0.88	0.93	0.26	0.21	0.17	1.01	0.11	0.24	0.12	0.19	0.2	0.17	0.15	0.00	0.42	1.59	1.03	2.27	2.17	1.32
Total	100.4	99.59	99.9	100.72	100.78	99.69	99.83	99.83	100.8	100.0	100.0	99.85	100.1	99.85	100.7	100.4	100.7	100.9	99.03	99.63	99.26	99.32	99.52

(1–3) gneissose granodiorites; (4–8) porphyroid granites; (9–15) leucocratic granites; (16–18) aplitic granites; (19, 20) garnet–biotite–anorthite–muscovite–quartz metasomatites from the marginal parts of the ore zone of the deposit; (21–23) tourmaline–garnet–muscovite–quartz metasomatites from the ore-bearing zone; the bold designates the samples used for the U–Pb isotopic investigations; (*) the analyses were performed using an S4 Pioneer X-ray fluorescence spectrometer designed by the Bruker AXS Company (DVGI DVO RAN, analyst E.A. Nozdrachev). The concentrations of the main petrogenic components in the other samples were determined by the standard chemical method (DVGI DVO RAN). (-) means not analyzed.

Table 2. Composition of the trace elements (ppm) in the granites of the Khaikta–Orogzhon massif and the metasomatites of the Berezitovoe deposit

Sample	@Bx-1	@Âõ-2	309	@Bx-3	356	4-A	8-1	65	8-2	16	1103	1267	1275
Ordered number	1	2	3	4	5	6	7	8	9	10	11	12	13
Be	1.6	2.1	2.2	1.5	1.4	2.4	2.7	2.2	2.1	1.1	1.6	0.7	1.7
Ba	1122.8	1156.8	923.8	1159.0	2123.0	447.6	346.2	315.3	189.1	111.1	144.8	69.1	564.3
Cs	0.8	1.4	0.5	1.9	1.0	3.4	1.9	3.0	1.3	1.3	0.8	0.8	1.2
Rb	58.1	119.3	89.8	156.3	132.8	203.7	242.5	200.6	276.6	179.2	218.6	118.76	206.5
Sr	883.1	474.0	568.1	326.7	296.6	84.3	126.0	100.6	37.3	14.5	13.7	5.1	46.9
Ga	19.7	17.9	18.0	17.6	14.8	17.4	20.3	18.1	20.7	17.4	19.5	11.3	26.1
Ta	1.1	0.7	0.8	0.8	0.6	0.9	1.0	0.8	1.2	0.6	0.8	0.4	1.7
Nb	14.7	10.0	13.2	9.7	8.2	10.3	14.1	10.5	17.8	9.2	13.6	5.0	27.9
Hf	6.8	4.9	4.3	4.9	2.1	4.3	5.8	4.6	6.6	4.2	7.0	2.0	12.6
Zr	264.2	173.7	162.9	173.4	72.9	153.9	217.9	167.5	238.7	157.2	263.6	87.8	508.7
Y	24.9	17.1	16.5	18.3	16.1	19.2	26.0	15.6	7.9	14.6	18.9	11.6	54.8
Th	15.3	10.0	7.5	10.6	5.4	11.8	25.2	13.2	21.8	9.8	23.2	5.8	28.4
U	2.9	2.4	2.1	5.7	1.1	3.8	6.5	4.4	4.7	2.5	3.3	1.3	6.6
Cr	21.5	12.4	14.2	12.3	11.9	10.8	9.2	6.6	6.0	35.0	17.9	10.6	197.6
Ni	12.4	8.8	11.2	12.4	10.7	8.9	8.3	6.3	3.0	5.4	14.5	9.3	12.6
Co	8.2	4.1	5.1	24.2	2.1	5.3	7.2	4.5	1.2	2.4	1.9	20.7	11.0
V	46.6	28.3	27.2	29.8	7.8	27.3	33.8	23.8	29.0	25.8	26.3	17.7	32.8
Pb	208.0	16.7	20.4	16.5	28.9	1396	259	62.3	38.0	2328.0	2713	810	230
Zn	65.3	341.5	42.5	460.9	28.5	975	1460	98.1	63.0	10106	5351	6086	443
Cd	0.00	0.00	0.00	0.00	0.00	2.47	4.25	0.25	0.50	45.14	24.35	24.12	5.10
Mo	1.66	1.28	0.87	3.37	0.94	1.70	3.40	1.35	0.76	3.71	1.05	0.87	29.73
Sn	18.03	3.30	1.73	1.86	1.64	7.03	1.45	1.51	1.59	5.37	6.76	3.05	3.40
W	1.50	5.06	2.70	32.18	1.90	7.90	10.65	9.37	17.42	9.73	13.20	21.03	25.78
La	50.34	34.66	22.35	42.06	15.39	50.69	63.99	31.53	23.10	28.28	52.24	15.58	77.19
Ce	100.3	67.89	48.22	77.24	24.64	94.54	130.24	61.19	40.40	52.44	97.04	30.23	157.29
Pr	10.88	7.62	6.07	8.17	2.75	10.43	14.10	6.78	4.02	5.56	9.80	3.18	17.81
Nd	41.57	27.55	20.82	29.37	10.93	37.66	51.68	24.11	13.56	19.05	33.17	11.44	66.88
Sm	7.40	4.65	3.95	5.03	2.31	6.54	8.48	4.05	2.02	3.26	5.05	1.84	12.03
Eu	1.66	1.19	0.95	1.17	0.60	1.49	1.78	0.95	0.57	0.76	0.89	0.28	2.25
Gd	6.72	4.50	3.37	4.69	2.70	5.99	8.23	3.96	1.71	3.32	4.93	2.04	12.09
Tb	0.90	0.59	0.48	0.66	0.47	0.77	1.05	0.51	0.26	0.50	0.59	0.32	1.75
Dy	5.12	3.57	2.92	3.43	2.68	3.94	5.39	2.93	1.25	2.80	3.41	1.93	10.57
Ho	1.00	0.65	0.55	0.67	0.63	0.79	1.08	0.57	0.34	0.57	0.75	0.43	2.19
Er	2.75	1.78	1.57	1.89	1.76	2.02	2.72	1.63	1.12	1.53	2.10	1.30	6.06
Tm	0.41	0.28	0.28	0.32	0.30	0.35	0.46	0.22	0.21	0.24	0.32	0.20	0.91
Yb	2.37	1.78	1.73	1.63	1.65	1.96	2.47	1.70	1.63	1.55	2.60	1.65	5.40
Lu	0.42	0.30	0.30	0.26	0.30	0.35	0.37	0.26	0.27	0.19	0.41	0.22	0.88
$(La/Yb)_n$	15.24	13.97	9.27	18.51	6.69	18.55	18.58	13.30	10.17	13.09	14.41	6.77	10.25
Eu/Eu*	0.71	0.78	0.78	0.72	0.73	0.71	0.64	0.72	0.91	0.70	0.54	0.44	0.56

(1–5) igneous rocks of the Khaikta–Orogzhon massif: (1–3) porphyroid granites, (4, 5) leucocratic granites; (6–13) metasomatites of the Berezitovoe deposit: (6–8) garnet-bearing metasomatites from marginal parts of the ore zone, (9–13) garnet-bearing muscovite–quartz metasomatites with sulfide mineralization. The bold font designates the samples used for the U–Pb isotopic investigations. $Eu/Eu^* = 2(Eu_n)/(Sm_n + Cd_n)$. The rocks were analyzed by the ICP-MS method using the Agilent 7500 spectrometer at the DVGI DVO RAN (analysts M.G. Blokhin and E.V. Elovskii).

Table 3. Results of the U–Pb isotopic investigations of the zircons from the granites and ore-bearing metasomatites of the Berezitovoe deposit (SHRIMP-II)

Analyzed points	$^{206}Pb_c$, %	U,ppm	Th, ppm	$^{206}Pb^*$, ppm	Isotopic ratios				Age, Ma		D,%
					$\frac{^{238}U}{^{206}Pb}$	$\frac{^{207}Pb}{^{206}Pb}$	$\frac{^{207}Pb}{^{235}U}$	$\frac{^{206}Pb}{^{238}U}$	$\frac{^{206}Pb}{^{238}U}$	$\frac{^{207}Pb}{^{235}U}$	
Porphyroid biotite–hornblende granite											
1.1	0.45	288	173	13.8	17.96 ± 1.5	0.0584 ± 4.8	0.420 ± 5.0	0.05567 ± 1.5	349.2 ± 5.1	356.1 ± 18	–2
1.2	0.31	448	323	21.0	18.39 ± 1.4	0.0572 ± 3.9	0.410 ± 4.1	0.05436 ± 1.4	341.3 ± 4.6	348.9 ± 14	–2
1.3	–	797	558	35.2	19.42 ± 1.3	0.0542 ± 2.5	0.392 ± 2.8	0.05151 ± 1.3	323.8 ± 4.0	335.8 ± 9	–4
1.4	0.32	687	429	32.2	18.39 ± 1.3	0.0569 ± 3.1	0.408 ± 3.4	0.05436 ± 1.3	341.2 ± 4.3	347.4 ± 12	–2
1.5	0.18	718	420	33.6	18.39 ± 1.3	0.0553 ± 2.5	0.404 ± 2.8	0.05438 ± 1.3	341.4 ± 4.3	344.5 ± 10	–1
1.6	0.24	797	506	38.1	18.02 ± 1.3	0.0563 ± 2.8	0.416 ± 3.1	0.05550 ± 1.3	348.2 ± 4.3	353.2 ± 11	–2
1.7	0.22	487	321	22.9	18.33 ± 1.4	0.0532 ± 3.4	0.387 ± 3.6	0.05455 ± 1.4	342.4 ± 4.5	332.2 ± 12	3
1.8	0.00	1464	838	90.0	13.98 ± 1.2	0.0573 ± 2.6	0.565 ± 2.9	0.07155 ± 1.2	445.5 ± 5.2	454.8 ± 13	–2
1.9	0.17	377	345	18.8	17.32 ± 1.7	0.0537 ± 3.1	0.416 ± 3.5	0.05774 ± 1.7	361.9 ± 5.8	353.2 ± 12	3
1.10	0.15	438	312	20.5	18.44 ± 1.4	0.0556 ± 2.8	0.406 ± 3.2	0.05423 ± 1.4	340.4 ± 4.7	346.0 ± 11	–2
Tourmaline–garnet–muscovite–quartz metasomatite											
3.1	–	939	725	46.8	17.20 ± 1.3	0.0540 ± 2.2	0.433 ± 2.5	0.05813 ± 1.3	364.2 ± 4.4	365.3 ± 9	0
3.2	0.21	738	740	34.7	18.32 ± 1.3	0.0552 ± 2.4	0.416 ± 2.8	0.05458 ± 1.3	342.6 ± 4.3	353.2 ± 10	–3
3.3	0.14	1185	945	51.9	19.63 ± 1.2	0.0532 ± 1.9	0.374 ± 2.3	0.05095 ± 1.2	320.4 ± 3.8	322.6 ± 7	–1
3.4	0.43	347	179	16.5	18.11 ± 1.5	0.0567 ± 4.2	0.431 ± 4.4	0.05520 ± 1.5	346.4 ± 4.9	363.9 ± 16	–5
3.5	0.91	310	178	14.2	18.89 ± 1.6	0.0567 ± 7.2	0.414 ± 7.4	0.05293 ± 1.6	332.5 ± 5.1	351.8 ± 26	–6
3.6	0.12	594	493	28.1	18.16 ± 1.3	0.0517 ± 2.8	0.393 ± 3.1	0.05507 ± 1.3	345.0 ± 4.5	336.6 ± 10	3
3.7	0.33	759	777	34.5	18.98 ± 1.3	0.0543 ± 3.3	0.395 ± 3.6	0.05270 ± 1.3	331.0 ± 4.2	338.0 ± 12	–2
3.8	0.62	472	220	22.3	18.29 ± 1.4	0.0543 ± 4.9	0.409 ± 5.1	0.05467 ± 1.4	343.1 ± 4.7	348.2 ± 18	–2
3.9	0.15	951	206	43.6	18.76 ± 1.3	0.0535 ± 2.1	0.393 ± 2.5	0.05330 ± 1.3	334.8 ± 4.1	336.6 ± 8	–1
3.10	0.32	447	386	20.5	18.84 ± 1.6	0.0515 ± 4.1	0.377 ± 4.4	0.05308 ± 1.6	333.4 ± 5.2	324.8 ± 14	3

The zircons were analyzed using the SHIMP-II high-resolution precision ion microprobe at the Center of Isotopic Investigations (VSEGEI). (Pb_c, Pb^*) the common and radiogenic constituents of the lead, respectively. The errors (%) are given for the interval of 1σ. The error of the standard calibration is 0.66%. The correction for common lead is given according to the measured ^{204}Pb. (D) is the discordance (wt %) = $(1 - {}^{207}Pb/{}^{235}U : {}^{206}Pb/{}^{238}U) \times 100$.

Table 4. Results of the U–Pb isotopic investigations of the zircons from the granites and ore-bearing metasomatites of the Berezitovoe deposit (LA-ICP-MS)

Analyzed points	Isotopic ratios (± %)			Age, Ma		D, %
	$^{207}Pb/^{206}Pb$	$^{207}Pb/^{235}Pb$	$^{206}Pb/^{238}U$	$^{207}Pb/^{235}U$	$^{206}Pb/^{238}U$	
Porphyroid biotite–hornblende granite						
2.1.r	0.06075 ± 8.71	0.48034 ± 6.59	0.06404 ± 2.26	398.3 ± 22	400.2 ± 8.8	0.5
2.2.r	0.06131 ± 13.51	0.38342 ± 8.22	0.05066 ± 2.78	329.6 ± 23	318.6 ± 8.7	–1
2.3.r	0.05960 ± 6.85	0.38031 ± 13.24	0.05169 ± 4.41	327.3 ± 37	324.9 ± 14	–1
2.4.r	0.05961 ± 7.36	0.38871 ± 6.52	0.05282 ± 2.23	333.4 ± 19	331.8 ± 7.2	–0.5
2.5.r	0.06013 ± 6.75	0.42178 ± 6.94	0.05682 ± 2.45	357.3 ± 21	356.3 ± 8.5	0
2.6.r	0.05927 ± 7.36	0.41601 ± 6.52	0.05685 ± 2.23	353.2 ± 19	356.5 ± 7.7	1
2.7.r	0.05568 ± 7.51	0.38035 ± 7.42	0.05533 ± 2.66	327.3 ± 21	347.2 ± 9.0	6
2.8.r	0.06038 ± 8.00	0.43531 ± 6.58	0.05840 ± 2.26	366.9 ± 20	365.9 ± 8.1	0
2.9.r	0.06029 ± 6.78	0.42153 ± 7.58	0.05663 ± 2.75	357.1 ± 23	355.1 ± 9.5	–0.5
2.10.r	0.05813 ± 7.04	0.38748 ± 6.70	0.05400 ± 2.31	332.5 ± 19	339.0 ± 7.6	2
2.11.z	0.06323 ± 5.3	0.44598 ± 5.0	0.05713 ± 2.0	374.5 ± 15.6	358.1 ± 6.9	–4
2.12.z	0.05834 ± 4.4	0.41209 ± 4.1	0.05722 ± 1.6	350.4 ± 12.1	358.7 ± 5.8	2
2.13.z	0.06095 ± 5.4	0.42497 ± 5.1	0.05648 ± 2.0	359.6 ± 15.4	354.2 ± 7.0	–2
2.14.z	0.06005 ± 5.3	0.41762 ± 5.0	0.05633 ± 2.0	354.3 ± 14.8	353.3 ± 6.8	0
2.15.z	0.05822 ± 4.4	0.41136 ± 4.1	0.05724 ± 1.7	349.9 ± 12.1	358.8 ± 5.8	2
2.16.z	0.06033 ± 5.8	0.40571 ± 5.4	0.05447 ± 2.1	345.8 ± 15.8	341.9 ± 7.2	–1
2.17.z	0.05992 ± 5.4	0.41387 ± 5.1	0.05595 ± 2.0	351.7 ± 15.1	350.9 ± 6.9	0
2.18.z	0.06036 ± 5.6	0.42255 ± 5.3	0.05671 ± 2.1	357.9 ± 16.0	355.6 ± 7.3	–0.5
2.19.z	0.05992 ± 5.7	0.41931 ± 5.3	0.05668 ± 2.1	355.6 ± 15.9	355.4 ± 7.3	0
2.20.z	0.05854 ± 4.4	0.41302 ± 4.1	0.05715 ± 1.6	351.0 ± 12.1	358.3 ± 5.7	2
2.21.z	0.11756 ± 5.3	3.28145 ± 4.9	0.22611 ± 2.0	1476.7 ± 38.3	1314.1 ± 23.4	–12
2.22.z	0.06011 ± 5.7	0.41455 ± 5.4	0.05586 ± 2.1	352.1 ± 16.0	350.4 ± 7.3	–1
2.24.z	0.12470 ± 5.4	5.05029 ± 5.0	0.32807 ± 2.1	1827.8 ± 42.5	1829.0 ± 32.9	0
Tourmaline–garnet–muscovite–quartz metasomatite						
4.1.r	0.05726 ± 3.4	0.37991 ± 3.2	0.05375 ± 1.7	327.0 ± 8.9	337.5 ± 5.55	3
4.2.r	0.05906 ± 3.9	0.37412 ± 3.6	0.05132 ± 1.9	322.7 ± 10.1	322.6 ± 5.85	0
4.3.r	0.06204 ± 3.5	0.38452 ± 3.3	0.05022 ± 1.7	330.4 ± 9.4	315.9 ± 5.33	4
4.4.r	0.07370 ± 4.5	0.28758 ± 4.2	0.03162 ± 2.0	256.7 ± 9.5	200.7 ± 3.94	–28
4.5.r	0.05817 ± 3.7	0.36203 ± 3.5	0.05044 ± 1.8	313.7 ± 9.5	317.2 ± 5.47	1
4.6.r	0.05861 ± 4.4	0.37683 ± 4.1	0.05210 ± 2.0	324.7 ± 11.5	327.4 ± 6.27	1
4.7.r	0.13769 ± 4.6	0.29976 ± 4.4	0.01764 ± 2.0	266.2 ± 10.2	112.7 ± 2.23	–135
4.8.r	0.05262 ± 4.7	0.34934 ± 4.5	0.05380 ± 2.0	304.2 ± 11.7	337.8 ± 6.73	10
4.9.r	0.07039 ± 4.9	0.48113 ± 4.7	0.05539 ± 2.2	398.8 ± 15.5	347.5 ± 7.33	–14
4.10.r	0.07577 ± 5.3	0.26361 ± 5.0	0.02819 ± 2.2	237.6 ± 10.6	179.2 ± 3.91	–33
4.11.z	0.05511 ± 1.11	0.43654 ± 1.03	0.05880 ± 0.41	368.5 ± 3.2	360.9 ± 1.5	–2
4.12.z	0.05340 ± 1.87	0.42611 ± 1.75	0.05787 ± 0.71	360.4 ± 5.3	362.6 ± 2.5	1
4.13.z	0.05274 ± 2.05	0.41673 ± 1.91	0.05730 ± 0.77	353.7 ± 5.7	359.2 ± 2.7	1
4.14.z	0.05412 ± 1.87	0.43611 ± 1.73	0.05845 ± 0.72	367.5 ± 5.3	366.2 ± 2.5	0
4.15.z	0.05381 ± 2.12	0.43437 ± 1.98	0.05855 ± 0.82	366.3 ± 6.1	366.8 ± 2.9	0
4.16.z	0.05377 ± 2.21	0.43311 ± 2.07	0.05842 ± 0.86	365.4 ± 6.4	366.0 ± 3.1	0
4.17.z	0.05657 ± 1.22	0.45656 ± 1.13	0.05853 ± 0.48	381.9 ± 3.6	366.7 ± 1.7	–4
418.z	0.05466 ± 1.92	0.43664 ± 1.79	0.05794 ± 0.74	367.9 ± 5.5	363.1 ± 2.6	–1
4.19.z	0.11460 ± 0.47	4.77802 ± 0.42	0.30240 ± 0.27	1781.0 ± 3.6	1703.2 ± 4.1	–5
4.20.z	0.11444 ± 0.75	4.19742 ± 0.68	0.26601 ± 0.43	1673.5 ± 5.6	1520.5 ± 5.8	–10
4.21.z	0.11290 ± 0.83	4.48620 ± 0.76	0.28820 ± 0.48	1728.4 ± 6.3	1632.5 ± 6.9	–6
4.22.z	0.11354 ± 1.06	5.18312 ± 0.96	0.33108 ± 0.61	1849.8 ± 8.2	1843.6 ± 9.9	0

(r) marginal parts of zircon grains; (z) cores of zircon grains. The errors of the individual analyses are 1σ. The errors of the standard calibration: TEMORA, 1.75%; 91500, 1.44%. (D) the discordance (wt %) = (1 – $^{207}Pb/^{235}U$: $^{206}Pb/^{238}U$) × 100. The zircon grains were analyzed at the Laboratory of Analytical Chemistry (DVGI DVO RAN) using an Agilent 7500a mass spectrometer with inductively coupled plasma combined with a UP-213 laser ablation system (analyst V.I. Kiselev).

single younger age estimates for the marginal parts of their grains: 276 ± 7, 208 ± 6, and 189 ± 7 Ma. According to the data obtained by the LA-ICP-MS method, the weighted average concordant age value calculated for eight data points is as old as 366 ± 2 Ma. The core areas of some zircon aggregates also yielded older dates: a concordant age of 1846.8 ± 9 Ma and discordant ages of 1742 ± 4, 1680 ± 7, and 1602 ± 5 Ma.

DISCUSSION

Before going to the geological interpretation of the obtained additional geochronnologic data, it is necessary to pay attention to the methodical aspects of this work since two different methods were used for the local measurements of the U–Pb isotopic ratios in the same zircon grains. In this connection, of particular interest is the comparison between the results obtained by these methods, since the SIMS method is widely used in Russia, while the LA-ICP-MS method is rarely applied for solving such gechronologic problems.

The comparison between the analytical potentials of the SIMS and the LA-ICP-MS methods reveals that the efficiency (the ratio between the detected ions and the total number of atoms received by the mass analyzer [41]) of the quadrupole mass spectrometer with laser ablation is lower as compared with that of the high-resolution secondary ion microprobe. The efficiency of the analytical system using the LA-ICP-MS method for measuring heavy masses is at the level of 0.04%, while this parameter for the SHRIMP-II method is equal to approximately 1% [40]. At the same time, the lower efficiency of the LA-ICP-MS method is partly compensated for by the higher level of the laser ablation of the material as compared with the ion microprobe, which results eventually in the higher sensitivity (the ratio between the counts per second (cps) and the concentration unit, i.e., usually ppm) of the plasma mass spectrometer with the laser ablation. The sensitivity of the LA-ICP-MS method with regard to ^{206}Pb is approximately 600 cps/ppm[1] with the ablation crater's diameter being 0.5–1.0 mm and 1800 cps/ppm with the ablation crater being 50 mm across, whereas the SHRIMP-II method is characterized by sensitivity of 0.8 cps/ppm for measuring a spot 25 mm across [40].

For measuring the U–Pb isotopic ratios by the LA-ICP-MS method, a material ablation rate of 0.5–1.0 μm/s is applied (with the repeated pulse frequency of 10 Hz), and the measurement duration is 100–120 sec, while, in the SHRIMP-II analysis, the ablation level is approximately 1 nm/s and the measurement usually lasts 15 min. Thus, the material discharged during the laser ablation is substantially higher as compared with that during the SHRIMP-II measurements (0.1–10.0 ppm vs. 2 ng, respectively), and the measurement itself is shorter.

The above-mentioned data (Figs. 9, 10) illustrate good consistency between the U–Pb ages obtained by the LA-ICP-MS and SIMS methods for the corresponding zones of the same zircon grains. Only two of ten grains extracted from the granite samples and analyzed by both dating methods yielded ages that substantially exceed the concordant values. This is explained by the capture of material from the zircon cores, which are characterized by relatively older age values (Figs. 9 C, 10 C; Tables 3, 4). The zircons from the ore-bearing metasomatites yielded concordant SHRIMP-II ages (Fig. 10 A, Table 3). At the same time, four crystals among these zircons provided inconsistent ages obtained by the analysis with laser ablation (Fig. 10 B, Table 4), which is probably determined by the lead loss or the material mixing from different growth zones.

Thus, the performed studies revealed that, despite the substantial differences between the SIMS and LA-ICP-MS methods, the last of them allows the U–Pb age to be estimated with accuracy comparable with that measured by the SHRIMP-II dating method. In this connection, it may be accepted that the dates obtained for the cores in the zircon grains by the LA-ICP-MS method are sufficiently reliable, which is important for the geological interpretation of the obtained isotopic data.

The results of the geochronologic investigations show that the igneous rocks of the Khaikta–Orogzhon massif most likely represent an autonomous complex of Late Paleozoic granitoids (more exactly, Early Carboniferous), not a constituent of the Early Proterozoic Late Stanovoi Complex. They provide the first reliable evidence indicating the Late Paleozoic magmatism in the eastern terminal part of the Selenga–Stanovoi orogenic belt.

In the opinion of some researchers, the earth's crust in the southeastern Siberian craton suffered considerable transformations in response to the widely developed tectono-metamorphic processes 1.9 Ga ago [5, 7], which determined the formation of the granitoid massifs of the Late Stanovoi and Tukuringra complexes. The Tukuringra granitoids were formed within the zones of the long-living faults of the Aldan–Stanovoi shield 1.88–1.86 Ga ago [21], which is confirmed by the U–Pb zircon ages of 1866 ± 95 [25] and 1840 ± 9 [10) Ma. The rocks of the Kengurak–Sergachi gabbro–anorthosite massif, fragments of which are widespread in the form of xenoliths among the granitoids of the Khaikta–Orogzhon massif, are 1866 ± 6 Ma old [2]. Our data show that the oldest ages determined for the cores of zircon grains from the granites of the Khaikta–Orogzhon massif (1828 ± 42 and 1846 ± 9 Ma) are consistent with the above-mentioned data

[1] The cps/ppm is the intensity of the signal (imp/s) generated by the detector during the analysis of a sample with the analyzed component content of 1 ppm (mg/l).

on the age of the granitization of the ancient granite–metamorphic complexes of the region under consideration obtained by other researchers. They are consistent with the general geological evolution of the region and reflect the Early Proterozoic stage of the regional metamorphism recorded in the rocks of the ancient crystalline basement.

Our additional geochronologic data indicate, along with the petrochemical and geochemical properties of the analyzed rocks, that the formation of the granitoids constituting the eastern terminal part of the Selenga–Stanovoi orogenic belt reflects the Hercynian tectono-magmatic cycle that was accompanied by the melting of the Precambrian crust and stimulated the formation of the palingenic granite massifs. The palingenic origin of the granites constituting the Khaikta–Orogzhon massif is confirmed by the hybridism and assimilation of the host metamorphic rocs of the Mogocha Group at the contact with the granites and by the rare older dates obtained for the zircon grain cores. This implies their formation on account of melted intensely metamorphosed rocks of the basement, which is in principle consistent with the traditional views on the nature of old magmatic complexes in the region.

In the Upper Amur region, manifestations of Paleozoic intrusive magmatism are documented in the eastern margin of the Argun superterrane. This area hosts small blocks of Early Paleozoic subalkaline leucocratic granites dated by the U–Pb method back to 467–472 Ma [28] and a system of small Late Paleozoic gabbro–diorite–granodiorite–granite massifs of the Urusha Complex, which are dated by the same method at 274–278 Ma [29]. According to the isotopic–geochemical properties, the rocks of the Urusha Complex correspond to *I*-type granites, which were formed in active continental crust settings. In the opinion of some researchers [1], the Late Paleozoic magmatism was responsible for the formation of a system of small gold ore occurrences represented by polysulfide–quartz and substantially quartz formations.

The paleozoic granitoids of the Olekma granite–leucogranite complex, which are widespread in the adjacent areas of the eastern Transbaikal region along the southeastern margin of the Selenga–Stanovoi belt spatially confined to the Mongol–Okhotsk suture zone are most probable analogs of the granites of the Khaikta–Orogzhon massif. The Olekma Complex includes massifs of porphyroid granodiorites, moderately acid granites, and leucogranites [3]. The calc-alkaline granitoids of this complex enclose abundant xenoliths of ancient gabbroids. The granites are palingenic in origin; they were formed on account of melted Precambrian metamorphic sequences that experienced ultrametamorphism. The age limits of the Olekma Complex are still ambiguous and debatable. At the same time, two periods are definable in the formation of the Paleozoic granitoids of the eastern Transbaikal region including the igneous rocks attributable to the Olekma Complex: the Early Paleozoic (476–431 Ma ago) and the Late Paleozoic (343–318 Ma ago) [16]. The terminal stage of the magamtism in the region is reflected in the formation of the intrusive granite–leucogranite massifs. The Zharcha massif located in the northern part of the Darasun gold ore deposit, which is dated by the Rb–Sr method back to 343 ± 7.6 Ma [15], is one of the typical representatives of the Olekma granite–leucogranite complex.

The Late Paleozoic igneous rocks of the western Transbaikal region represented by widespread calc-alkaline and alkaline granitoids constituting the Mongol–Transbaikal belt are investigated in more detail. It is assumed that the Late Paleozoic magmatism in this region occurred at the postcollisional (330–310 Ma ag) and intraplate (285–275 Ma ago) stages of the Hercynian cycle [35, 36]. The early stage of the Late Paleozoic magmatism was marked by the formation of the Barguzin Complex represented by high-K calc-alkaline granites that constitute the large Angara–Vitim batholith [26, 36]. A particular feature of the granitoids characteristic of this stage is their autochthonous formation from the melted host granite gneisses.

The presented data show that the dates obtained for the Khaikta–Orogzhon massif of the Upper Amur region correspond to the ages obtained for the Paleozoic granitoids from the western part of the Selenga–Stanovoi orogenic belt. Noteworthy is some similarity between the obtained dates and the age of the known Angara–Vitim batholith. Our data allow the assumption that the granitoids of the Khaikta–Orogzhon massif represent one of the eastern fragments of a single belt of Late Paleozoic magmatism within the Selenga–Stanovoi orogenic belt. The late Paleozoic magmatism marked the collisional stage of the region's development at the beginning of the Mongol–Okhotsk ocean's closure [13, 14, 27] or reflected the interaction between the continental crust and the large mantle plumes of the North Asian thermal field [38].

By their U–Pb ratios, the zircons from the metasomatites of the ore zone are relatively close to their counterparts from the host granites. Moreover, it is revealed that the core parts of the zircon grains from the igneous rocks and the metasomatites contain relict protozircons with close concordant ages of 1828 Ma (for the granites) and 1846 Ma (for the metasomatites). At the same time, the zircon grains from the ore-bearing metasomatites are characterized by the more significant difference between the ages obtained for their cores and marginal parts (366–323 Ma) and the single dates corresponding to younger model ages.

The close ages established for the zircons from the porphyroid granites (344–355 Ma) and the metasomatites of the Berezitovoe deposit (323–366 Ma) unambiguously indicate that the host porphyroid granites of the Khaikta–Orogzhon massif served as a source for the ore-bearing metasomatic rocks of the deposit. It should be emphasized that no substantial changes in the isotopic composition of the zircons at the stage of the metasomatic transformations and the subsequent ore formation are documented.

CONCLUSIONS

(1) The results of the U–Pb investigations of the same single zircon grains by the SIMS (Center of Isotopic Investigations, VSEGEI) and LA-ICP-MS (DVGI DVO RAN) methods are compared. It is shown that the method of the mass spectrometry combined with laser ablation, which is rarely used in Russia, offers the opportunity to reliable estimate the U–Pb ages of the rocks, and the accuracy is comparable with that of the SHRIMP-II data.

(2) According to the U–Pb isotopic zircon dating by the SIMS and LA-ICP-MS methods, the porphyroid granitoids of the Khaikta–Orogzhon massif that host the ore body of the Berezitovoe deposit were formed 344–355 Ma ago. These data represent the first evidence in favor of the Hercynian magmatism's manifestation in the eastern part of the Selenga–Stanovoi orogenic belt.

(3) The single older dates obtained for cores of zircon grains with concordant ages of 1828–1846 Ma indicate, along with the available geological and geochemical data, the palingenic origin of the granitoids of the Khaikta–Orogzhon massif and their formation on account of the melted host metamorphic rocks of the Mogocha Group during the Hercynian tectonomagmatic cycle in the development of the Selenga–Stanovoi belt.

(4) The Late Paleozoic granitoids of the Olekma and Barguzin complexes of the eastern and western Transbaikal region are probable close-age analogs of the granites in the Khaikta–Orogzhon massif of the Upper Amur region. This allows the granitoids of the Khaikta–Orogzhon massif to be considered as constituting the eastern fragment of the belt characterized by the development of the Late Paleozoic magmatism along the southeastern margin of the North Asian craton.

(5) The Paleozoic age of the granitoids in the Khaikta–Orogzhon massif makes it possible to outline some similarity between the geological structures of the Berezitovoe gold–polymetallic deposit of the Upper Amur region and the Darasun gold ore deposit of the eastern Transbaikal region, where the coeval structurally and compositionally close igneous rocks of the Krestovskii and Olekma complexes constitute the largest part of the ore field.

(6) The occurrence of zircon grains with ages of 323–366 Ma in the ore-bearing tourmaline–garnet–muscovite–quartz rocks of the Berezitovoe deposit unambiguously indicates that the granites of the Khaikta–Orogzhon massif served as the primary protolith for the formation of the metasomatites of this ore object.

ACKNOWLEDGMENTS

We are grateful to the administration and geological personnel of the Open Joint Stock Company Berezitovyi Rudnik Ltd. for their assistance in conducting the field works on the deposit, as well as to the reviewers V.V. Akinin and A.M. Spiridonov for their criticism and recommendations, which promoted the improvement of the manuscript and the better interpretation of the original data. This work was supported by the Far East Branch of the Russian Academy of Sciences (project nos. 12-III-A-08-145, 12-II-A-08-146, and 12-II-SO-08-030).

REFERENCES

1. I. V. Buchko and A. A. Sorokin, "Late Paleozoic magmatic arc on the northern periphery of the Argun terrane and associated gold mineralization, Upper Amur region," Russ. Geol. Geophys. **46** (6), 617–624 (2005).
2. I. V. Buchko, E. B. Sal'nikova, A. A. Sorokin, et al., "First age and geochemical data on the rocks of the Kengurak–Sergachin gabbro-anorthosite massif, southeastern framing of the Siberian craton," Tikhookean. Geol. **25** (2), 15–23 (2006).
3. I. A. Vasil'ev, V. P. Kapanin, G. P. Kovtonyuk, et al., *Raw-Mineral Base of the Amur District on the Turn of Centuries* (Blagoveshchensk, 2000) [in Russian].
4. A. S. Vakh, V. A. Stepanov, and O. V. Avchenko, "Beresite gold–polymetallic deposit: geological structure and ore composition," Rudy Met., No. 6, 44–55 (2008).
5. S. N. Gavrikova, L. L. Nikolaeva, A. V. Galanin, et al., *Early Precambrian of the Southern Stanovoy Folded Area* (Nedra, Moscow, 1991) [in Russian].
6. *Geodynamics, Magmatism, and Metallogeny of East Russia*, Ed. by A. I. Khanchuk (Dal'nauka, Vladivostok, 2006) [in Russian].
7. *Geological Map of the Amur Region and Adjacent Territories. 1 : 2500000. Explanatory Note*, Ed. by L. I. Krasnyi, A. S. Vol'skii, Pen Yun'byao, et al., (St. Petersburg–Blagoveshchensk–Harbin, 1999) [in Russian].
8. V. A. Glebovitsky, I. S. Sedova, D. I. Matukov, et al., "Age of the Stanovoy Complex of East Siberia: evidence from SHRIMP II ion microprobe data," Dokl. Earth Sci. **412** (3), 35–38 (2007).
9. V. Goroshko, V. B. Kaplun, and Yu. F. Malyshev, "Dzheltulak Fault: deep structure, evolution, and metallogeny," Litosfera, No. 6, 38–54 (2010).
10. V. A. Gur'yanov, G. V. Roganov, V. N. Zelepugin, et al., "Isotopic–geochronological studies of zircons from the Early Precambrian rocks of the southeastern Aldan–Stanovoy Shield: new results and their geological interpretation," Russ. J. Pac. Geol. **6** (2), 97–113 (2012).
11. G. S. Gusev and V. E. Khain, "Relations of the Baikal-Vitim, Aldan-Stanovoy, and Mongol-Okhotsk terranes

(southern Middle Siberia),” Geotektonika, No. 5, 68–82 (1995).

12. *Precambrian Geology of USSR,* Ed. by D. V. Runqkvist and F. P. Mitrofanov (Nauka, Leningrad, 1988) [in Russian].
13. L. P. Zonenshain, M. I. Kuzmin, and L. M. Natapov, *Tectonics of the Lithospheric Plates of the USSR Territory* (Nedra, Moscow, 1990), Vol. 1 [in Russian].
14. Yu. G. Zorin, V. G. Belichenko, E. Kh. Turutanov, et al., “Terranes of Eastern Mongolia and Central Transbaikalia and development of the Mongol-Okhotsk fold belt,” Geol. Geofiz. **39** (1), 11–25 (1998).
15. M. E. Kazimirovskii, S. I. Dril’, and G. P. Sandimirova, “Comparative geochemistry and age of the Paleozoic granitoids of the Western Stanovoy Zone of Transbaikalia,” Geol. Geofiz. **41** (7), 900–1002 (2000).
16. M. E. Kazimirovskii, G. P. Sandimirova, and E. V. Bankovskaya, “Isotope geochronology of the Paleozoic granitoids of the Selenga–Stanovoy Mountainous Area,” Geol. Geofiz. **43** (11), 973–989 (2002).
17. T. V. Kaulina, Extended Abstract of Doctoral Dissertation in Geology and Mineralogy (Apatity, 2011).
18. V. I. Kiselev, G. M. Vovna, M. A. Mishkin, and E. Yu. Kovaleva, “Simultaneous single-grain determination of trace element abundances and U/Pb isotope ratios in zircons by LA-ICP-MS,” in *Proceedings of 8th Scientific Conference “Analytics of Siberia and Far East”, Tomsk, Russia, 2008* (Tomsk, 2008), pp. 78–79 [in Russian].
19. Z. P. Kozak and K. D. Vakhtomin, *State Geological Map of the Russian Federation. 1 : 200000. 2-nd Ed. Stanovaya Series. N-51-XIV (Takhtamygda)* (VSEGEI, St. Petersburg, 2000) [in Russian].
20. Z. P. Kozak, S. N. Belikov, and M. N. Shilova, *State Geological Map of the Russian Federation. 1 : 200000. 2nd Ed. Zeiskaya Series. Sheet N-51-XXII*, Ed. by L. P. Korsakova (VSEGEI, St. Petersburg, 2002) [in Russian].
21. A. B. Kotov, Extended Abstract of Doctoral Dissertation in Geology and Mineralogy (St. Petersburg, 2003).
22. A. M. Larin, A. B. Kotov, E. B. Sal’nikova, et al., “New data on the age of granites of the Kodar and Tukuringra complexes, Eastern Siberia: geodynamic constraints,” Petrology **8** (3), 238–248 (2000). 1
23. A. M. Larin, A. B. Kotov, E. B. Sal’nikova, et al., “Mesozoic granites of the Chubachin Massif, Tukuringra Complex, Dzhugdzhur–Stanovoi foldbelt: new geochemical, geochronological, and isotopic–geochemical evidence,” Petrology **9** (4), 362–375 (2001).
24. A. M. Larin, E. B. Sal’nikova, A. B. Kotov, et al., “Late Archean granitoids of the Dambukinski Block of the Dzhugdzhur–Stanovoy fold belt: formation and transformation of the continental crust in the Early Precambrian,” Petrology **12** (3), 211–226 (2004).
25. A. M. Larin, E. B. Sal’nikova, A. B. Kotov, et al., “Early Cretaceous age of regional metamorphism of the Stanovoi Group in the Dzhugdzhur–Stanovoi foldbelt: geodynamic implications,” Dokl. Earth Sci. **409** (2), 727–731 (2006). 1
26. A. M. Mazukabzov, T. V. Donskaya, I. P. Gladkochub, and I. P. Paderin, “The Late Paleozoic geodynamics of the West Transbaikalian segment of the Central Asian fold belt,” Russ. Geol. Geophys. **51** (5), 482–491 (2010).
27. L. M. Parfenov, N. A. Berzin, A. I. Khanchuk, et al., “Genetic model of the orogenic belts of the northeastern Asia,” Tikhookean. Geol. **22** (6), 7–41 (2003).
28. A. A. Sorokin, N. M. Kudryashov, Li Jinyi, D. Z. Zhuravlev, et al., Early Paleozoic granitoids in the eastern margin of the Argun Terrane, Amur area: first geochemical and geochronologic data," Petrology **12** (4), 367–376.
29. A. A. Sorokin, A. B. Kotov, N. M. Kudryashov, and V. P. Kovach, “Late Paleozoic Urusha magmatic complex in the southern framing of the Mongolia–Okhotsk Belt (Amur Region): age and geodynamic setting,” 1 Petrology **13** (6), 596–610 (2005).
30. V. A. Stepanov, A. V. Mel’nikov, A. S. Vakh, et al., *Amur Gold Province* (AmGU, NIGTTs DVO RAN, Blagoveshchensk, 2008) [in Russian].
31. A. M. Strelov, *Geological Map of the USSR. 1 : 200 000. Sheet N-50-XXXII* (Moscow, 1981) [in Russian].
32. V. E. Strikha, N. N. Petruk, K. D. Vakhtomin, et al., “Geology of the Khaikta intrusive complex (Upper Amur Region),” Tikhookean. Geol. **19** (5), 25–37 (2000).
33. *Tectonics, Deep Structure, and Metallogeny of the Junction Zone between the Central–Asian and Pacific belts: explanatory note to the tectonic map. 1 : 1500000*, Ed. by L. P. Korsakov, Yu. F. Malyshev, and M. V. Goroshko (DVO RAN, Khabarovsk–Vladivostok, 2005) [in Russian].
34. O. M. Turkina, A. D. Nozhkin, and T. B. Bayanova, “Sources and formation conditions of Early Proterozoic granitoids from the southwestern margin of the Siberian Craton,” Petrology **14** (3), 262–283 (2006).
35. A. A. Tsygankov, D. I. Matukov, N. G. Berezhnaya, et al., “Late Paleozoic granitoids of western Transbaikalia: magma sources and stages of formation,” Russ. Geol. Geophys. **48** (1), 120–140 (2007).
36. A. A. Tsygankov, B. A. Litvinovskii, B. M. Jahn, et al., “Sequence of magmatic events in the Late Paleozoic of Transbaikalia, Russia (U-Pb isotope data),” Russ. Geol. Geophys. **51** (9), 972–994 (2010).
37. *Evolution of the Early Precambrian Lithosphere of the Aldan–Olekma–Stanovoy Region* (Nauka, Leningrad, 1987) [in Russian].
38. V. V. Yarmolyuk and V. I. Kovalenko, “Deep geodynamics and mantle plumes: their role in the formation of the Central Asian fold belt,” Petrology **11** (6), 504–531 (2003).
39. L. P. Black, S. L. Kamo, G. M. Aleinikoff, et al., “TEMORA 1: a new zircon standard for Phanerozoic U-Pb geochronology,” Chem. Geol. **200**, 155–170 (2003).
40. W. Compston, “Geological age by instrumental analysis. The 29th Halmond lecture,” Mineral. Mag. **63**, 297–311 (1999).
41. I. Horn, R. L. Rudnick, and W. F. McDonough, “Precise elemental and isotope ratio determination by simultaneous solution nebulization and laser ablation-ICP-MS: application to U-Pb geochronology,” Chem. Geol. **167**, 405–425 (2000).

42. S. E. Jackson and W. L. Griffin, et al., "The application of laser ablation-inductively coupled plasma-mass spectrometry to in situ U/Pb zircon geochronology," Chem. Geol. **211**, 47–69 (2004).

43. K. R. Ludwig, "ISOPLOT EX. Version 2.06. A geochronological toolkit for Microsoft Excel," Berkeley Geochronol. Center Spec. Publ., No. 1a, (1999).

44. K. R. Ludwig, "SQUID 1.00 users manual," Berkeley Geochronol. Center, Spec. Publ., No. 2, (2000).

45. W. F. McDonough and S. Sun, "The composition of the Earth," Chem. Geol. **120**, 223–253 (1995).

46. R. L. Rudnick and S. Gao, "Composition of the Continental Crust," in *The Crust* (Elsevier-Pergamon, Amsterdam, 2003), Vol. 3, pp. 1–64.

47. J. B. Whalen, K. L. Currie, and B. W. Chappel, "A-type granites: geochemical characteristics, discrimination and petrogenesis," Contrib. Mineral. Petrol. **95**, 407–419 (1987).

48. J. B. Whalen, V. J. McNicoll, C. R. van Staal, et al., "Spatial, temporal, and geochemical characteristics of Silurian collision-zone magmatism, Newfoundland Appalachians: an example of a rapidly evolving magmatic system related to slab break-off," Lithos **89**, 377–404 (2006).

49. D. G. Whiterford, I. A. Nicholls, and S. R. Taylor, "Spatial variations in the geochemistry of Quaternary lavas across the Sunda Java and Bali," Contrib. Mineral. Petrol. **70**, 341–356 (1979).

50. M. Wiedenbeck, P. Alle, F. Corfu, et al., "Three natural zircon standards for U-Th-Pb, Lu-Hf, trace element and REE analyses," Geostand. News **19**, 1–23 (1995).

51. I. S. Williams, "Applications of microanalytical techniques to understanding mineralizing processes," Rev. Econ. Geol. **7**, 1–35 (1998).

Recommended for publishing by N.A. Goryachev

Translated by I. Basov

SPELL: 1. geodynamic